Smart Structures and Systems, *Vol. 27, No. 3 (2021) 447-455*
DOI: https://doi.org/10.12989/sss.2021.27.3.447

Seismic isolation of railway bridges using a self-centering pier

Xiushen Xia, Xiyin Zhang*, Jun Shi and Jingyao Tang

School of Civil Engineering, Lanzhou Jiaotong University, Lanzhou, 730070, China

(*Received October 15, 2019, Revised September 22, 2020, Accepted December 9, 2020*)

Abstract. Earthquakes cause severe damages to bridge structures, and rocking isolation of piers has become a superior option for the seismic protection of bridges during earthquakes. A seismic isolation method with free rocking mode is proposed for railway bridge piers with medium height. Experimental and numerical analysis are conducted to evaluate the seismic performance of the rocking-isolated bridge pier. Shaking table test is carried out with a scaled model by using three strong input earthquake records. The measured data includes displacement, acceleration and time history response of the pier-top and the bending moment of the pier-bottom. Test results show that the expected uplift and rocking of the isolated pier occur under strong earthquakes and the rocking-isolated pier has self-centering capacity. Slight damage appears at the collision surface between pier and base due to pier uplift, while there is no damage in the pier body. The bending moment of pier-bottom is less affected by the spectrum of input ground motions. The two-spring model is provided to simulate the isolated pier with free rocking mode under earthquakes. A seismic response analysis model for the rocking-ioslated pier is established with the assistance of OpenSees platform. The simulated results agree well with the measured results by shaking table test. Therefore, the seismic isolation method with a self-centering pier is worthy of promotion for railway bridges in high seismic risk regions.

Keywords: seismic isolation; railway bridges; free rocking mode; self-centering pier; shaking table test and numerical simulation

1. Introduction

Bridges form crucial links in the transportation network especially in high seismic risk regions (Iranmanesh *et al*. 2009), and seismic damages can cause massive loss. Seismic isolation method with self-adaptive centering system is an option to mitigate seismic damage of bridges subjected to earthquakes (Liu *et al*. 2011, Wei *et al*. 2019, Zheng *et al*. 2019). The base isolation techniques represent an interesting design strategy for decoupling the structure from the damaging effects due to ground accelerations in case of seismic events (Cancellara and De Angelis 2017). Rocking during an earthquake is common for free-standing objects and also for many other engineering systems (Diamantopoulos and Fragiadakis 2019). The rocking pier system (RPS) allows the columns to rock on beam or foundation surfaces during the attacks of a strong earthquake (Cheng and Chen 2014). Therefore, the rocking isolation is a most attractive alternative for the seismic protection of bridges.

For a long time, the research of rocking isolation mostly concentrates on the rocking vibration of rigid body (Taniguchi 2002, Palmeri and Makris 2008, Vassiliou and Makris 2012, Bachmann *et al*. 2017). Rocking idea in seismic design of bridges was first carried out in 1970s, and rocking isolation has been applied in the South Rangitikei railway bridge in New Zealand (Beck and Skinner 1973). In the 1990s, the rocking concept was regarded as an effective method for seismic strengthening of bridges (Priestley *et al*. 1996). Through a series of reduced-scale shaking table tests, Anastasopoulos *et al*. (2013) found that rocking isolation is quite effective in reducing the inertia forces transmitted onto the superstructure of bridges, hence the rocking-isolated pier is effectively protected. The seismic isolation bridge with rocking pier is also accompanied by footing uplift during earthquakes. Chen *et al*. (2017) presented the results of free vibrations and shake table tests on a single degree-of-freedom model of a bridge pier with footing uplift on a rigid base. A self-centering designed double-column pier was presented by Cheng (2008), and shaking table test results showed that the bridge model rocked up to at least 5% of the column rotation without damage or residual deformation.

The concept of hybrid system, where self-centering and energy dissipation capacity are adequately combined by using unbonded post-tensioned techniques and alternative sources of dissipation, has been recently proposed as a viable and efficient solution for an improved seismic performance of bridge systems (Palermo *et al*. 2007, Palermo and Pampanin 2008). Solberg *et al*. (2009) also used the damage avoidance design philosophy in rocking bridge piers by steel–steel armored interfaces during rocking. Compared with conventional cast-in-place RC piers, the rocking pier has better self-centering ability and significantly reduces bridge pier damage. The prestressed rocking piers with built-in energy-dissipating devices under earthquakes have less damage, but the energy-dissipating steel bars are seriously damaged and difficult to replace

*Corresponding author, Associate Professor,
E-mail: zhangxiyin@mail.lzjtu.cn

http://www.techno-press.org/?journal=sss&subpage=7
ISSN: 1738-1584 (Print), 1738-1991 (Online)

after the earthquake. The external energy-dissipating device instead of the built-in energy-dissipating device is applied in the non-bonded prestressed rocking pier. These external energy-dissipating devices can effectively protect the pier and act as a fuse unit, and it is very convenient to replace after the earthquake (Chou and Chen 2006, Marriott *et al.* 2009, 2011).

The concept of using pier rocking for seismic isolation of bridge structures has been demonstrated feasible. A series of tests by using scaled-down model structures of a typical viaduct pier system show that the rocking pier system (RPS) for seismic protection of viaduct pier structures is effective and stable (Chen *et al.* 2006). For bridge piers with spread footing foundations, the rocking isolation effect also resulted in an increase in the displacement response at the deck's level, especially in the case of near fault ground motions (Hung *et al.* 2011). Roh and Reinhorn (2010) found that the increased displacements of rocking concrete columns can be controlled by using supplemental viscous dampers. Rocking piers can limit the seismic damage and residual displacement under strong earthquakes to maintain the post-earthquake serviceability of bridges (Zhou *et al.* 2019). The rocking bridge with freestanding columns presented excellent post-earthquake resilience and serviceability after earthquakes with limited damage and negligible residual displacement (Du *et al.* 2019, Rele *et al.* 2019). Thomaidis *et al.* (2020) pointed out that the bridge isolated with free-rocking pier is susceptible to a failure mode related to the abutment-backfill system, which can occur prior to the well-known overturning of the rocking pier.

As stated above, previous researches on seismic isolation method with rocking pier have been done in recent years. However, the center of gravity of the existing self-centering pier is close to the support point during rocking, thus the free-rocking pier will be prone to overturning if the pier height increases to medium or more. It is unfavourable for rapid construction if the constraint components are used to prevent overturning. In this study, a simple and useful free-rocking isolation mode for the medium-height pier with pile foundations was designed by the separation of the pier and pile foundation at the pile cap. The pier is self-centering and the center of gravity of pier is far away from the support point after the earthquake, which can improve the anti-overturning stability of pier in rocking isolation under strong earthquakes. Scaled models of free rocking-isolated pier and non-ioslation pier based on a simple supported beam bridge are fabricated and shaking table tests of scaled models are carried out to investigate the seismic response of the isolation effect. A two-spring model is presented for the rocking-isolated pier and numerical analysis is performed with the assistance of OpenSees platform.

2. Design of the rocking-isolated pier

In order to prevent the pier and the foundation from damage by rocking isolation under strong earthquakes. A free-rocking isolation mode for the bridge pier of medium or more height was proposed, as seen in Fig. 1.

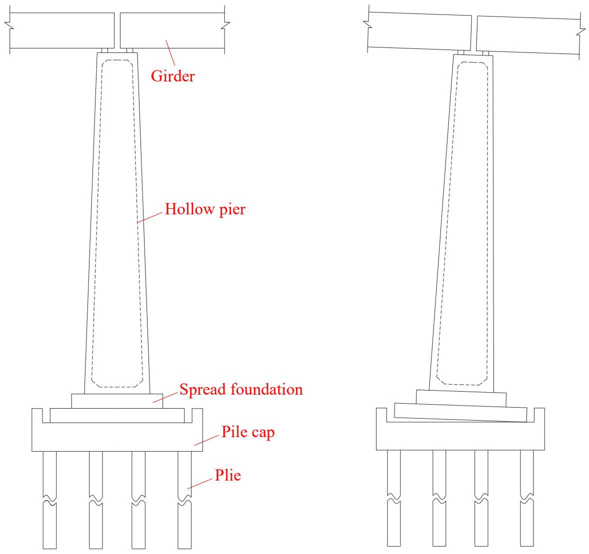

(a) Stable stage (b) Rocking stage

Fig. 1 Rocking isolated bridge pier with pile foundation

In Fig. 1, the isolation surface is located between the spread foundation at the pier-bottom and the pile cap. When lifting up, the center of gravity of the pier system is far from the lifting support point, and the pier has better stability in the rocking isolation. The free rocking isolation pier is similar to the spread foundation pier on the traditional rock foundation. The difference is that the free rocking piers are allowed to lift off under strong earthquakes. When the bridge pier is in normal service and under frequent earthquake, the vertical load is used to balance the horizontal load so that the rocking-isolated pier keeps stable (see Fig. 1(a)). The stability bending moment of the pier is calculated according to Eq. (1) and Fig. 2. Uplift of the rocking-isolated pier is not expected under normal service loads and frequent earthquakes. Therefore, calculation and evaluation are needed includes the resultant force eccentricity of the base of the spread foundation, the strength of the foundation the anti-sliding and anti-overturning stability.

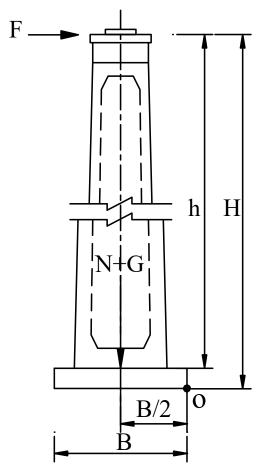

Fig. 2 Calculation diagram of stability moment

$$M_y = (N + G) \cdot \frac{B}{2} \tag{1}$$

In Fig. 2 and Eq. (1), N is the supporting force of the pier top; G is the self-weight of the pier body; B is the calculated direction to spread base width associated with the pier body; H is the height of the pier body.

Under the strong earthquake, when the seismic moment of the pier bottom exceeds the stable bending moment M_y at the bottom of the pier, the pier is uplift and rocking (Fig. 1(b)), and the pier is freely rocking to achieve the purpose of isolation.

3. Shaking table test of the free rocking isolated pier

3.1 Model bridge construction and experiment design

A hollow bridge pier with a height of 38m on Dali-Ruili railway in China is used as prototype. The reinforcement ratio of longitudinal reinforcement is 0.8%, the diameter of stirrup is 12 mm, the spacing of stirrups is 10 cm, and the volume stirrup ratio is 0.9%. The superstructure of the bridge is a simply supported T-beam of post tensioned prestressed concrete. The span of the simply supported beam is 32 m, and the dead load of a single span is 518.28 t. The geometric similarity ratio of the model pier is determined to be 1/25. The main similitude ratio of the model is shown in Table 1.

A HW350×350 standard H-beam with a length of 5 m and a mass of 663 kg was used to simulate the superstructure. The total height of the model pier is 1.82 m (excluding the base), wherein the pier height is 1.52 m, the pier section is 20 cm (loading direction) × 27 cm (out-of-plane), and the upper and lower layers are 40c m (loading direction) × 47 cm (out-of-plane) × 15 cm (vertical) and 60 cm × 67 cm × 15 cm, see Fig. 3. In the model pier, HRB335 longitudinal steel bars for 8Φ10 are arranged, and the full-section reinforcement ratio is 1.16%. The rocking isolation pier and the non-rocking isolation pier were designed in the same structural dimensions. The base was designed as a reinforced concrete pedestal of 80 cm × 80 cm × 10 cm, and a steel plate having a thickness of 2 cm was set around and the bottom. The size and reinforced configuration design of the model pier are shown in Fig. 3.

Table 1 Similitude ratio between model and prototype pier

Quantities	Calculation formula	Scaling factor
Length S_L	(Control constant)	1/25
Modulus of elasticity S_E	(Control constant)	1
Acceleration S_a	(Control constant)	1
Mass S_m	$S_m = S_E S_L^2/S_a$	0.0016
Stress S_σ	$S_\sigma = S_E$	1
Strain S_ε	$S_\varepsilon = 1$	1
Displacement S_u	$S_u = S_L$	1/25

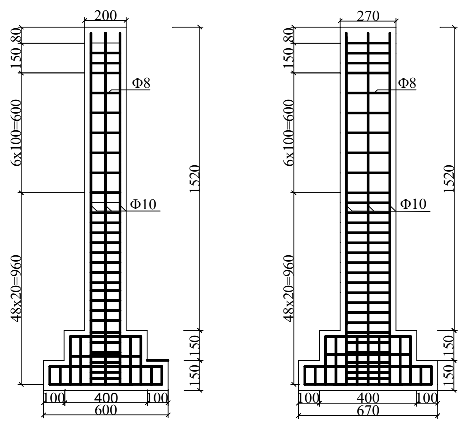

Fig. 3 The size and reinforced configuration design of the model pier

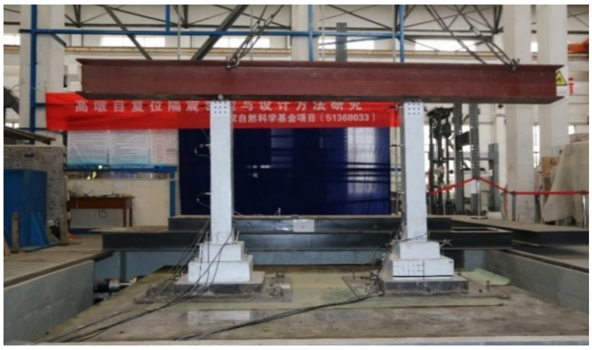

Fig. 4 Arrangement of the shaking table test

The base of the model pier was fixed at the shaking table by connecting bolts. During testing, the free-rocking pier can rock on the base, while the non-rocking pier was fixed at the base. The main beam was connected with the rocking pier by a fixed bearing, and the support pier was connected by a movable bearing. The entire inertial force of the main beam was applied to the rocking pier. The arrangement of the shaking table test is shown in Fig. 4.

In order to ensure the safety of the shaking table test and prevent the main beam from falling off and damaging the shaking table, one end of the cable was connected to the crane and the other end was connected to the H-section steel beam. When the H-beam is not detached, the steel cable is in an unstressed state and have no additional effect on the test.

The main purpose of the test is to observe the phenomenon of uplift, rocking and self-centering of free-rocking piers and to obtain seismic response analysis data. The test results can be used to verify the numerical analysis model for free-rocking. The excitation direction of the test is to input the ground motion in the horizontal direction.

Test instruments such as acceleration sensors, displacement sensors and strain gauges were arranged on the free-rocking model pier (see Fig. 5). In Fig. 5, the letter A represents the acceleration sensor, D represents the displacement sensor, the arrow represents the recording direction, and the alphanumeric characters in the brackets represent the number of the acceleration sensing in the non

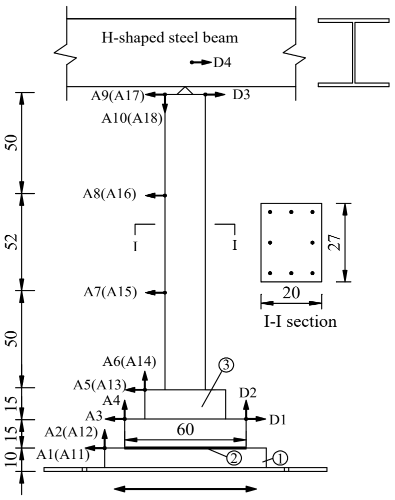

Fig. 5 Structure of pier and arrangement of measure points (unit: cm)

rocking pier. ①—model base; ②—lifting surface; ③—spread foundation connected to the pier.

3.2 Test results and analysis

The 1940 El-Centro strong earthquake record was selected as the ground motion input. In order to investigate the influence of the seismic spectrum, the far field 1985 Mexico strong earthquake record and the near-field 1999 Chi-Chi strong earthquake record were also selected as the ground motion input. The seismic information is listed in Table 2. The acceleration amplitudes of the three seismic waves were adjusted to a uniform value after input.

The seismic wave was applied as input along the bridge. The free-rocking pier started to uplift at the separation surface when the PGA of the El-Centro wave was 0.15 g. When the PGA increased to 0.20 g, the free-rocking pier had obvious uplift, the beam body oscillated with rocking. The displacement of the pier top along the bridge is significant. There were similar experimental phenomena under the excitation of the Mexico wave and the Chi-Chi wave. Among them, the displacement of the pier top along the bridge is particularly obvious under the excitation of the Mexico wave. During the test, no slippage occured at the bottom of the pier when the pier was rocking. The isolated pier showed rocking vibration. After the earthquake, the pier was self-centering, and the lifting surface was slightly damaged. No visible cracks appeared in the pier.

White noise sweeping was carried out before and after the test. The fundamental frequency obtained before the test is 5.25 Hz, and the damping ratio is 9.1%. After the test, the fundamental frequency of the rocking pier is 4.56 Hz, and the damping ratio is 9.3%. After the test, the base frequency of the pier decreased slightly and the damping increased slightly compared with that before the test. The displacement and acceleration response of pier top under three seismic waves are listed in Table 3.

The ratio of the measured acceleration peak of each measuring point of the pier to the actual peak of the acceleration on the table is recorded as the acceleration reaction amplification factor K. The acceleration response amplification curves of the free-rocking pier under the three input ground motions are shown in Fig. 6.

As can be seen from Fig. 6, the *K* values of free-rocking pier under different types of the earthquake excitation with PGA of 0.20 g have a slight difference below 80 mm, and the difference become larger over 80 mm in pier height. The maximum *K* value under Chi-Chi wave excitation is 9.1, more than twice that under El-Centro wave and Mexico wave excitation. While maximum *K* values under El-Centro wave and Mexico wave excitation are more than twice that under Chi-Chi wave excitation. For El-Centro and Mexico waves, the acceleration in the middle of the pier is greater than that at the top and bottom of the pier, and the acceleration at the two measuring points above the pier is close to each other. The acceleration of Chi-Chi wave pier increases approximately linearly with the pier height.

Table 2 Selected ground motions

Ground motions	Station	Magnitude	PGA/g	PGV/cm.s^{-1}	PGD/cm
1940 Imperial Valley	El centro	7.0	0.313	29.8	13.32
1999 Chi-Chi	CHY101	7.6	0.44	115.0	68.75
1985 Mexico	-	8.1	0.039	10.3	28.53

Table 3 Main test results

Load condation	Wave	PGA/g	Fundamental frequency /Hz	Damping /%	Pier top		Base moment/ (kN.m)
					Displacement /mm	Acceleration /(m.s^{-2})	
1	white noise	0.07	5.25	9.1	-	-	-
2	El-Centro	0.20	—	—	22.3	6.6	1.86
3	Mexico	0.20	—	—	41.2	6.9	1.76
4	Chi-Chi	0.20	—	—	21.7	17.6	1.60
5	white noise	0.07	4.56	9.3	-	-	-

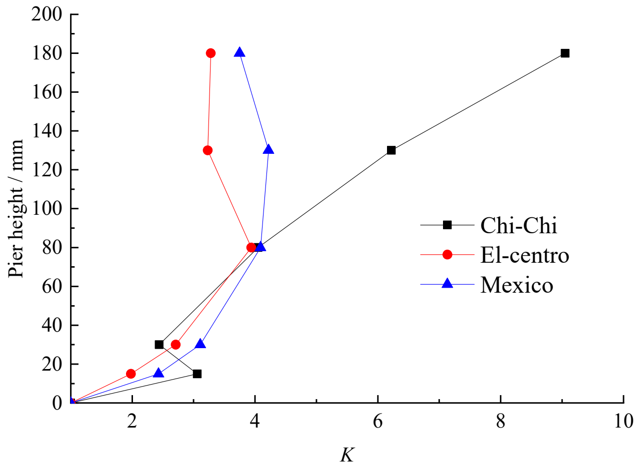

Fig. 6 Relationship between ground motion types and K

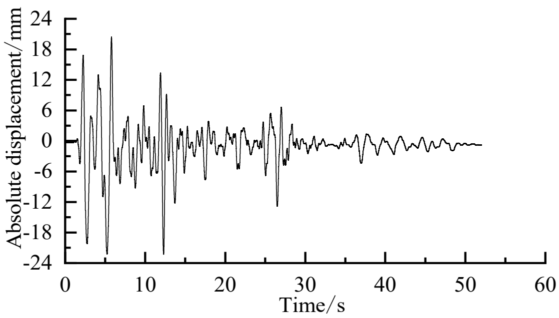

Fig. 7 Time history of pier-top displacement

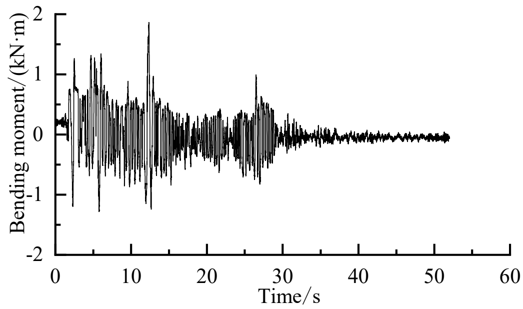

Fig. 8 Time history of base moment

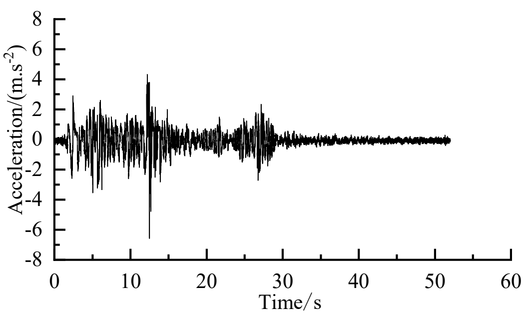

Fig. 9 Time history of pier-top acceleration

Table 3 shows that the displacement response of the pier top under the action of the far-field Mexico wave is the largest and significantly larger than that of the near-field Chi-Chi wave and the ordinary ground motion El-Centro wave. The acceleration of the pier top under the action of the near-field Chi-Chi wave is the largest, which is much larger than the top acceleration of the other two waves. The common ground motion El-Centro wave has the largest bending moment response. The top displacement of the El-Centro wave is similar to that of the Chi-Chi wave. The bending moments of the piers under the action of three waves have no significant difference from each other. This indicates that the bending moment at the bottom of the free-rocking pier is less affected by the spectrum of the input ground motion.

The time-history response curves of the rocking response of the free-rocking bridge piers under three input ground motions were obtained. The time history curves of the pier-top displacement, the pier-bottom bending moment (base moment) and the pier-top acceleration obtained by the experiment with the PGA of 0.2 g under El-Centro wave are shown in Figs. 7-9.

4. Two-spring model for free rocking isolated pier

In order to simulate the free rocking and uplift of the pier, the two-spring finite element analysis model was adopted (Yim and Chopra 1984), as shown in Fig. 10. In the model, the elastic beam element was used to simulate pier, concentrate mass was used to simulate bridge span weight, rigid arm element was used to simulate pier bottom spread foundation, fundamental mass accumulates at the center of spread foundation, and the only compressed spring was used to simulate pier uplift. Rayleigh damping $[C] = \alpha[M] + \beta[K]$ was adopted in the model, and the same damping ratio was used in the calculation of coefficients α and β.

It is assumed that stiffness is independent of natural frequency, the vertical stiffness of rectangular rigid foundation on half-space foundation is approximately expressed as follows.

$$K_v = \frac{4GR_0}{1-\nu} \tag{2}$$

$$R_0 = \sqrt{A_0/\pi} \tag{3}$$

The compressive stiffness of the spring at each end of the two-spring model is the half of the basic vertical stiffness, as shown in Eq. (4).

$$k = \frac{1}{2}K_v \tag{4}$$

In Eq. (4) and Fig. 10, where k is the lift-off spring stiffness; K_v is the basic vertical stiffness; R_0 is the equivalent radius; A_0 is the cross-sectional area of the base of the pier.

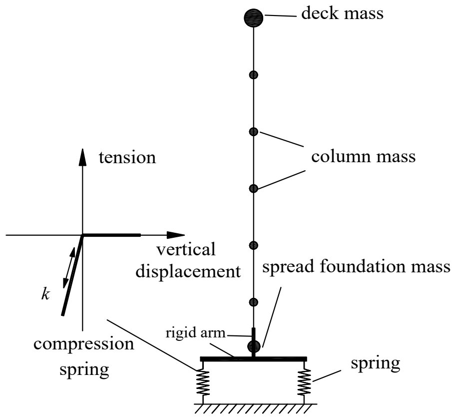

Fig. 10 Two-spring model for rocking-isolated pier

5. Numerical simulation of the free rocking isolated pier

The dimensions of the test model bridge are shown in Fig. 11. The two-spring model is used for numerical simulation of the seismic response of the free rocking pier. The concrete elastic modulus E of the model pier is 3.30×10^6 MPa, the shear modulus G is 1.42×10^6 MPa, Poisson's ratio is 0.2, and the model uplift spring stiffness k calculated by Eqs. (2) to (4) is 1.27×10^6 kN/m. The mass of the pier is the mass of all beams: 0.663 t. The vertical force of the pier is the reaction force of the beam at the top of the free rocking bridge: 4.5 kN. In the numerical simulation analysis of the free-rocking isolated bridge, the free-rocking vibration response of the simply supported beam is simplified to the vibration response of the free-rocking pier according to the boundary support and the pier top constraint.

With assistance of the OpenSees platform, the widely-used open-source computational platform (Kolozvari *et al.* 2018), a numerical model for the free rocking isolated pier was established. Both the pier and the rigid arm were simulated by the Elastic-Beam-Column element. The stiffness of the rigid arm is 100 times of the maximum stiffness of the element. The uplift spring element was simulated by Zero-Length Element with the elastic non-tensile uniaxial Material ENT material. The beam mass was simulated by a mass unit and applied to the pier top. The vertical force of the pier top had an effect on the stable bending moment, which was applied by the nodal force.

The horizontal displacement of pier-top, bending moment of pier-bottom and acceleration time history curve of pier-top under El-Centro wave with PGA of 0.2 g were plotted in Figs. 12-14. From Fig. 12, it can be seen that the time history curve of numerical simulation of pier-top displacement coincides well with that of test results. This indicates that the two-spring numerical analysis model can reflect the displacement response of free-rocking pier well. The same trend is also seen in the displacement response under Mexico wave and Chi-Chi wave excitation.

Fig. 13 shows that the numerical simulation time-history curve of the bending moment of the pier is in good agreement with the time-history curve of the test results. This indicates that the two-spring numerical analysis model also can reflect the bending moment response of the free-rocking pier. The other two waves also have this rule.

From Fig. 14, it can be seen that there are obvious differences between the test results of pier-top acceleration and those of calculated results at about 12 s. From the shape of the time history curve, except for the abnormal points of about 12 s, the time history curves of pier-top acceleration numerical simulation agree well with the time history curves of test results during the whole loading process. An abnormal point also occurs at around 12 s for the acceleration curve measured by the shaking table test, which is much larger than the numerical simulation result at the same time. This indicates that the two-spring numerical analysis model can reflect the acceleration response of the free-rocking pier as a whole, but differences appear at the maximum value between the simulated and test results. Because the maximum acceleration measured in the test includes the collision between the free rocking pier and the uplift surface. Otherwise, the external environmental noise can also influence the maximum value of the test results.

Since there are many factors affecting the acceleration, in order to further examine the two-spring analysis model, the numerical simulation analysis results of the pier-top

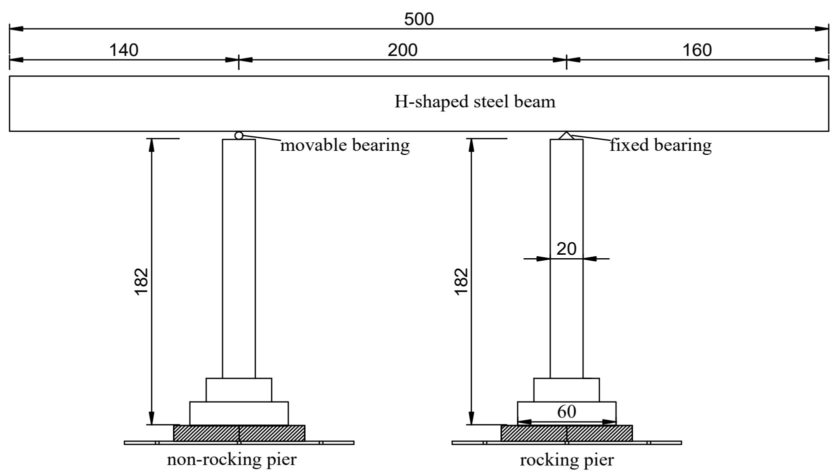

Fig. 11 Bridge schematic of model (unit: cm)

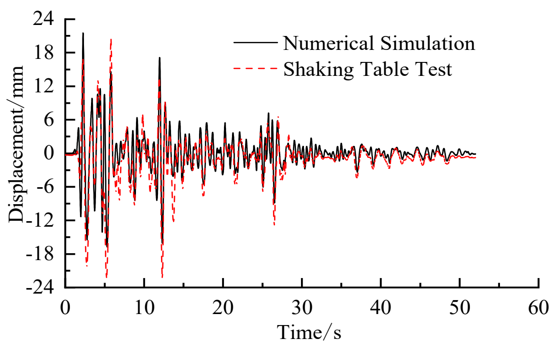

Fig. 12 Comparisons between calculated and test values of pier-top displacement

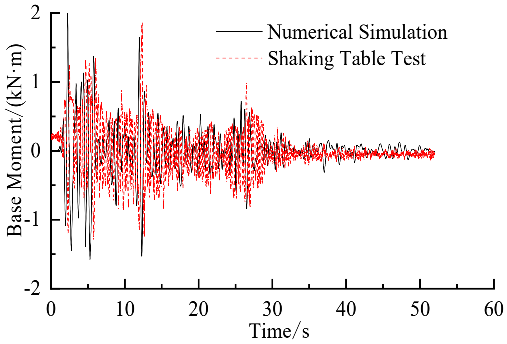

Fig. 13 Comparisons between calculated and test values of pier-bottom bending moment

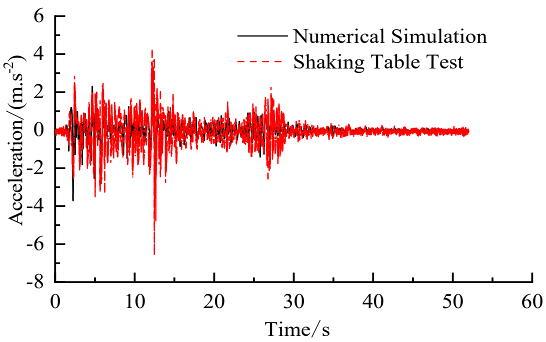

Fig. 14 Comparisons between calculated and test values of pier-top acceleration

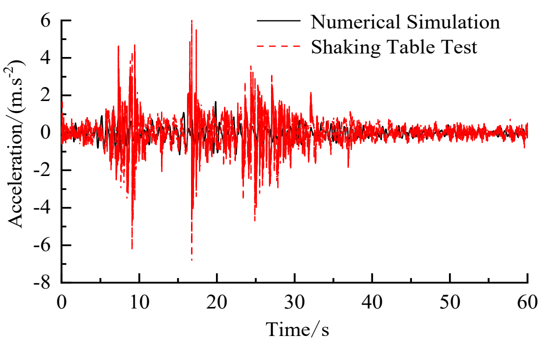

Fig. 15 Comparisons between calculated and experimental values of pier top acceleration

acceleration response under the far-field Mexico wave are shown in Fig. 15. From Fig. 15, it can be found that the numerical simulation results of Mexico wave under far-field ground motion are the same as El-Centro wave. There is a great difference between the two-spring model and shaking table test when it is used to simulate pier top acceleration.

Based on the test and numerical analysis results, the maximum pier-top displacement is less than 24 mm, the ratio between the pier-top displacement and the pier height is less than 1.6%. It can ensure the pier to stay stable during earthquakes. It is also shown that the base moment of the isolated pier is less than 2 kN·m, which indicates that the free-rocking pier has excellent seismic isolation performance.

6. Conclusions

The use of free-rocking pier is a low-cost and easy-construction method for seimic isolation of bridges. If the pier height increases to a medium or more, the free rocking pier will be prone to overturning under earthquakes. In this study, a free rocking isolation method for railway bridge piers with medium height was proposed, and verified by shaking table test and numerical analysis. The main conclusions are as follows.

- Shaking table test results showed that the expected uplift and rocking isolation of the designed isolated pier occur under strong earthquakes, but no horizontal slip at the pier footing. After the earthquake, the rocking pier is completely self-centering and slight damage appears at the uplift and collision position, and there is no damage in the pier
- It can be found that the pier-top displacements of the free rocking isolated pier under the far field, near-field and ordinary ground motion are quite different, but the pier-bottom bending moments are relatively close. This indicated that the displacement and acceleration of the pier top of the free rocking isolation bridge are greatly affected by the spectral characteristics of the input ground motion, while the bending moment of the pier bottom is less affected.
- The time-history curve of the pier-top displacement and pier-bottom bending moment from numerical analysis agree well with the time-history curve obtained by the shaking table test. It can be concluded that the two-spring model provided in this study can better simulate the seismic responses of the free rocking isolated pier for railway bridges.

However, we found that there exist differences between the measured and calculated time-history curves of the pier-top acceleration. Therefore, the two-spring numerical analysis model cannot be used to simulate the pier-top acceleration response of the free-rocking isolation pier. Thus, more experiments and numerical analysis are still needed for widespread application with confidence.

Acknowledgments

This research is supported by the National Natural Science Foundation of China (Grant No. 51668035, 51808273, 52068041 and 52068045), Project funded by China Postdoctoral Science Foundation (for Xiyin Zhang), Science and Technology Program of Gansu Province for Distinguished Young Scholars (Grant No. 20JR5RA430), Youth Talent Support Project of China Association for Science and Technology (for Xiyin Zhang), Tianyou Youth Talent Lift Program of Lanzhou Jiaotong University (Xiyin Zhang) and lzjtu (201801) EP support. On behalf of all authors, the corresponding author states that there is no conflict of interest.

References

Anastasopoulos, I., Loli, M., Georgarakos, T. and Drosos, V. (2013), "Shaking table testing of rocking—isolated bridge pier on sand", *J. Earthq. Eng.*, **17**(1), 1-32. https://doi.org/10.1080/13632469.2012.705225

Bachmann, J.A., Strand, M., Vassiliou, M.F., Broccardo, M. and Stojadinovic, B. (2017), "Is rocking motion predictable?", *Earthq. Eng. Struct. Dyn.*, **47**(2), 535-552. https://doi.org/10.1002/eqe.2978

Beck, J.L. and Skinner, R.I. (1973), "The seismic response of a reinforced concrete bridge pier designed to step", *Earthq. Eng Struct. Dyn.*, **2**(4), 343-358. https://doi.org/10.1002/eqe.4290020405

Cancellara, D. and De Angelis, F. (2017), "Assessment and dynamic nonlinear analysis of different base isolation systems for a multi-storey RC building irregular in plan", *Comput. Struct.*, **180**, 74-88. https://doi.org/10.1016/j.compstruc.2016.02.012

Chen, Y.-H., Liao, W.-H., Lee, C.-L. and Wang, Y.-P. (2006), "Seismic isolation of viaduct piers by means of a rocking mechanism", *Earthq. Eng. Struct. Dyn.*, **35**(6), 713-736. https://doi.org/10.1002/eqe.555

Chen, Y., Larkin, T. and Chouw, N. (2017), "Experimental assessment of contact forces on a rigid base following footing uplift", *Earthq. Eng. Struct. Dyn.*, **46**(11), 1835-1854. https://doi.org/10.1002/eqe.2885

Cheng, C.-T. (2008), "Shaking table tests of a self-centering designed bridge substructure", *Eng. Struct.*, **30**(12), 3426-3433. https://doi.org/10.1016/j.engstruct.2008.05.017

Cheng, C.-T. and Chen, F.-L. (2014), "Seismic performance of a rocking bridge pier substructure with frictional hinge dampers", *Smart Struct. Syst., Int. J.*, **14**(4), 501-516. https://doi.org/10.12989/sss.2014.14.4.501

Chou, C.-C. and Chen, Y.-C. (2006), "Cyclic tests of post-tensioned precast CFT segmental bridge columns with unbonded strands", *Earthq. Eng. Struct. Dyn.*, **35**(2), 159-175. https://doi.org/10.1002/eqe.512

Diamantopoulos, S. and Fragiadakis, M. (2019), "Seismic response assessment of rocking systems using single degree-of-freedom oscillators", *Earthq. Eng. Struct. Dyn.*, **48**(7), 689-708. https://doi.org/10.1002/eqe.3157

Du, X.-L., Zhou, Y.-L., Han, Q. and Jia, Z.-L. (2019), "Shaking table tests of a single-span freestanding rocking bridge for seismic resilience and isolation", *Adv. Struct. Eng.*, **22**(15) 3222-3233. https://doi.org/10.1177/1369433219859410

Hung, H.-H., Liu, K.-Y., Ho, T.-H. and Chang, K.-C. (2011), "An experimental study on the rocking response of bridge piers with spread footing foundations", *Earthq. Eng. Struct. Dyn.*, **40**(7), 749-769. https://doi.org/10.1002/eqe.1057

Iranmanesh, A., Bassam, A. and Ansari, F. (2009), "Post earthquake performance monitoring of a typical highway overpass bridge", *Smart Struct. Syst., Int. J.*, **5**(4), 495-505. https://doi.org/10.12989/sss.2009.5.4.495

Kolozvari, K., Orakcal, K. and Wallace, J.W. (2018), "New opensees models for simulating nonlinear flexural and coupled shear-flexural behavior of RC walls and columns", *Comput. Struct.*, **196**, 246-262. https://doi.org/10.1016/j.compstruc.2017.10.010

Liu, J.-L., Zhu, S., Xu, Y.-L. and Zhang, Y. (2011), "Displacement-based design approach for highway bridges with SMA isolators", *Smart Struct. Syst., Int. J.*, **8**(2), 173-190. https://doi.org/10.12989/sss.2011.8.2.173

Marriott, D., Pampanin, S. and Palermo, A. (2009), "Quasi-static and pseudo-dynamic testing of unbonded post-tensioned rocking bridge piers with external replaceable dissipaters", *Earthq. Eng. Struct. Dyn.*, **38**(3), 331-354. https://doi.org/10.1002/eqe.857

Marriott, D., Pampanin, S. and Palermo, A. (2011), "Biaxial testing of unbonded post-tensioned rocking bridge piers with external replacable dissipaters", *Earthq. Eng. Struct. Dyn.*, **40**(15), 1723-1741. https://doi.org/10.1002/eqe.1112

Palermo, A. and Pampanin, S. (2008), "Enhanced seismic performance of hybrid bridge systems: comparison with traditional monolithic solutions", *J. Earthq. Eng.*, **12**(8), 1267-1295. https://doi.org/10.1080/13632460802003819

Palermo, A., Pampanin, S. and Marriott, D. (2007), "Design, modeling, and experimental response of seismic resistant bridge piers with posttensioned dissipating connections", *J. Struct. Eng.*, **133**(11), 1648-1661. https://doi.org/10.1061/(ASCE)0733-9445(2007)133:11(1648)

Palmeri, A. and Makris, N. (2008), "Linearization and first-order expansion of the rocking motion of rigid blocks stepping on viscoelastic foundation", *Earthq. Eng. Struct. Dyn.*, **37**, 1065-1080. https://doi.org/10.1002/eqe.799

Priestley, M.J.N., Seible, F. and Calvi, G.M. (1996), *Seismic Design and Retrofit of Bridge*, John Wiley & Sons, Inc.

Rele, R.R., Dammala, P.K., Bhattacharya, S., Balmukund, R. and Mitoulis, S. (2019), "Seismic behaviour of rocking bridge pier supported by elastomeric pads on pile foundation", *Soil Dyn. Earthq. Eng.*, **124**, 98-120. https://doi.org/10.1016/j.soildyn.2019.05.018

Roh, H. and Reinhorn, A.M. (2010), "Modeling and seismic response of structures with concrete rocking columns and viscous dampers", *Eng. Struct.*, **32**(8), 2096-2107. https://doi.org/10.1016/j.engstruct.2010.03.013

Solberg, K., Mashiko, N., Mander, J.B. and Dhakal, R.P. (2009), "Performance of a damage-protected highway bridge pier subjected to bidirectional earthquake attack", *J. Struct. Eng.*, **135**(5), 469-478. https://doi.org/10.1061/(ASCE)0733-9445(2009)135:5(469)

Taniguchi, T. (2002), "Non-linear response analyses of rectangular rigid bodies subjected to horizontal and vertical ground motion", *Earthq. Eng. Struct. Dyn.*, **31**(8), 1481-1500. https://doi.org/10.1002/eqe.170

Thomaidis, I.M., Kappos, A.J. and Camara, A. (2020), "Dynamics and seismic performance of rocking bridges accounting for the abutment-backfill contribution", *Earthq. Eng. Struct. Dyn.*, **49**(12), 1161-1179. https://doi.org/10.1002/eqe.3283

Vassiliou, M.F. and Makris, N. (2012), "Analysis of the rocking response of rigid blocks standing free on a seismically isolated base", *Earthq. Eng. Struct. Dyn.*, **41**(2), 177-196. https://doi.org/10.1002/eqe.1124

Wei, B., Li, C., Jia, X., He, X. and Yang, M. (2019), "Effects of shear keys on seismic performance of an isolation system", *Smart Struct. Syst., Int. J.*, **24**(3), 345-360.

https://doi.org/10.12989/sss.2019.24.3.345
Yim, S.C.S. and Chopra, A.K. (1984), "Dynamics of Structures on two-spring foundation allowed to uplift", *J. Eng. Mech.*, **110**(7), 1124-1146.
https://doi.org/10.1061/(ASCE)0733-9399(1984)110:7(1124)
Zheng, Y., Dong, Y., Chen, B. and Anwar, G.A. (2019), "Seismic damage mitigation of bridges with self-adaptive SMA-cable-based bearings", *Smart Struct. Syst.*, *Int. J.*, **24**(1), 127-139.
http://dx.doi.org/10.12989/sss.2019.24.1.127
Zhou, Y.-L., Han, Q., Du, X.-L. and Jia, Z.-L. (2019), "Shaking table tests of post-tensioned rocking bridge with double-column bents", *J. Bridge Eng.*, **24**(8), 04019080.
https://doi.org/10.1061/(ASCE)BE.1943-5592.0001456

HJ